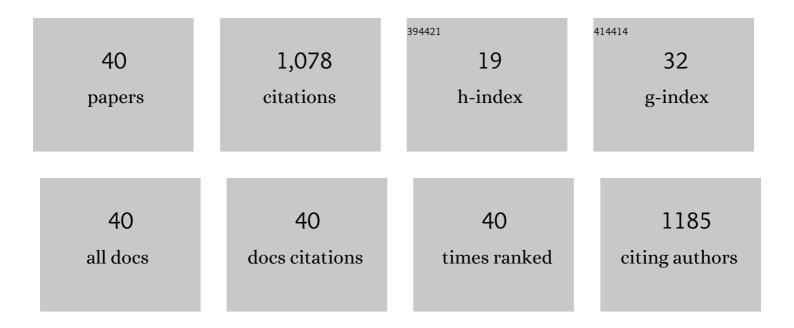
Hougang Fan

List of Publications by Year in descending order

Source: https://exaly.com/author-pdf/2940770/publications.pdf Version: 2024-02-01



Ηομέλνε Γλν

#	Article	IF	CITATIONS
1	Monitoring the charge-transfer process in a Nd-doped semiconductor based on photoluminescence and Applications, 2020, 9, 117.	16.6	111
2	Optimized design of three-dimensional multi-shell Fe3O4/SiO2/ZnO/ZnSe microspheres with type II heterostructure for photocatalytic applications. Applied Catalysis B: Environmental, 2018, 227, 61-69.	20.2	88
3	ZnO nanoparticles on MoS2 microflowers for ultrasensitive SERS detection of bisphenol A. Mikrochimica Acta, 2019, 186, 593.	5.0	47
4	One-pot synthesis of ZnS nanowires/Cu ₇ S ₄ nanoparticles/reduced graphene oxide nanocomposites for supercapacitor and photocatalysis applications. Dalton Transactions, 2019, 48, 2442-2454.	3.3	46
5	SERS polarization-dependent effects for an ordered 3D plasmonic tilted silver nanorod array. Nanoscale, 2018, 10, 8106-8114.	5.6	44
6	Eco-friendly nanostructured Zn–Al layered double hydroxide photocatalysts with enhanced photocatalytic activity. CrystEngComm, 2019, 21, 4607-4619.	2.6	42
7	The study of structural and optical properties of (Eu, La, Sm) codoped ZnO nanoparticles via a chemical route. Materials Chemistry and Physics, 2017, 194, 29-36.	4.0	40
8	Charge Transfer in an Ordered Ag/Cu ₂ S/4-MBA System Based on Surface-Enhanced Raman Scattering. Journal of Physical Chemistry C, 2018, 122, 5599-5605.	3.1	40
9	AgNPs decorated Mg-doped ZnO heterostructure with dramatic SERS activity for trace detection of food contaminants. Journal of Materials Chemistry C, 2019, 7, 8199-8208.	5.5	40
10	In-situ surface-enhanced Raman scattering based on MTi20 nanoflowers: Monitoring and degradation of contaminants. Journal of Hazardous Materials, 2021, 412, 125209.	12.4	40
11	Recyclable Magnetic MIP-Based SERS Sensors for Selective, Sensitive, and Reliable Detection of Paclobutrazol Residues in Complex Environments. ACS Sustainable Chemistry and Engineering, 2020, 8, 14549-14556.	6.7	39
12	2D MOF-derived porous NiCoSe nanosheet arrays on Ni foam for overall water splitting. CrystEngComm, 2021, 23, 69-81.	2.6	37
13	Highly enhanced photocatalytic properties of ZnS nanowires–graphene nanocomposites. RSC Advances, 2014, 4, 30798-30806.	3.6	36
14	Carrier Density-Dependent Localized Surface Plasmon Resonance and Charge Transfer Observed by Controllable Semiconductor Content. Journal of Physical Chemistry Letters, 2018, 9, 6047-6051.	4.6	36
15	Activating Old Materials with New Architecture: Boosting Performance of Perovskite Solar Cells with H ₂ Oâ€Assisted Hierarchical Electron Transporting Layers. Advanced Science, 2019, 6, 1801170.	11.2	35
16	Site-selective growth of Ag nanoparticles controlled by localized surface plasmon resonance of nanobowl arrays. Nanoscale, 2019, 11, 6576-6583.	5.6	34
17	Zinc oxide nanotubes decorated with silver nanoparticles as an ultrasensitive substrate for surface-enhanced Raman scattering. Mikrochimica Acta, 2012, 179, 315-321.	5.0	25
18	Ultrasound-assisted synthesis of hyper-dispersed type-II tubular Fe3O4@SiO2@ZnO/ZnS core/shell heterostructure for improved visible-light photocatalysis. Journal of Alloys and Compounds, 2020, 838, 155689.	5.5	24

HOUGANG FAN

#	Article	IF	CITATIONS
19	Synthesis and photoluminescence characterizations of the Er 3+ -doped ZnO nanosheets with irregular porous microstructure. Materials Science in Semiconductor Processing, 2016, 41, 32-37.	4.0	20
20	Self-cleaning semiconductor heterojunction substrate: ultrasensitive detection and photocatalytic degradation of organic pollutants for environmental remediation. Microsystems and Nanoengineering, 2020, 6, 111.	7.0	20
21	Enhanced semiconductor charge-transfer resonance: Unprecedented oxygen bidirectional strategy. Sensors and Actuators B: Chemical, 2021, 327, 128903.	7.8	19
22	Structure evolution of chromium-doped boron clusters: toward the formation of endohedral boron cages. RSC Advances, 2019, 9, 2870-2876.	3.6	18
23	Improved Charge Transfer and Hot Spots by Doping and Modulating the Semiconductor Structure: A High Sensitivity and Renewability Surface-Enhanced Raman Spectroscopy Substrate. Langmuir, 2019, 35, 8921-8926.	3.5	18
24	Destroying the symmetric structure to promote phase transition: Improving the SERS performance and catalytic activity of MoS2 nanoflowers. Journal of Alloys and Compounds, 2021, 886, 161268.	5.5	18
25	Mesoporous TiO ₂ coated ZnFe ₂ O ₄ nanocomposite loading on activated fly ash cenosphere for visible light photocatalysis. RSC Advances, 2018, 8, 1398-1406.	3.6	17
26	Tuning red emission and photocatalytic properties of highly active ZnO nanosheets by Eu addition. Journal of Luminescence, 2018, 204, 573-580.	3.1	16
27	Carrier dynamic monitoring of a π-conjugated polymer: a surface-enhanced Raman scattering method. Chemical Communications, 2020, 56, 2779-2782.	4.1	16
28	XPS and Raman study of the active-sites on molybdenum disulfide nanopetals for photocatalytic removal of rhodamine B and doxycycline hydrochlride. RSC Advances, 2018, 8, 36280-36285.	3.6	15
29	Synthesis, characterization and photoluminescence property of La-doped ZnO nanoparticles. Applied Physics A: Materials Science and Processing, 2016, 122, 1.	2.3	13
30	Construction of an MZO heterojunction system with improved photocatalytic activity for degradation of organic dyes. CrystEngComm, 2020, 22, 7059-7065.	2.6	13
31	Plasmon-coupled Charge Transfer in FSZA Core-shell Microspheres with High SERS Activity and Pesticide Detection. Scientific Reports, 2019, 9, 13876.	3.3	11
32	Interface synthesis of MoS2@ZnO@Ag SERS substrate for the ultrasensitive determination of bilirubin. Applied Surface Science, 2022, 598, 153750.	6.1	11
33	Increasing local field by interfacial coupling in nanobowl arrays. RSC Advances, 2017, 7, 43671-43680.	3.6	10
34	Visible-light-driven photocatalytic degradation of RhB by carbon-quantum-dot-modified g-C ₃ N ₄ on carbon cloth. CrystEngComm, 2021, 23, 4782-4790.	2.6	10
35	A novel strategy for improving SERS activity by cerium ion fÂ→Âd transitions for rapid detection of endocrine disruptor. Chemical Engineering Journal, 2022, 430, 131467.	12.7	8
36	Fabrication and adsorption properties of multiwall carbon nanotubes-coated/filled by various Fe3O4 nanoparticles. Journal of Materials Science: Materials in Electronics, 2019, 30, 18802-18810.	2.2	7

HOUGANG FAN

#	Article	IF	CITATIONS
37	Oxygen vacancy induced electron traps in tungsten doped Bi ₂ MoO ₆ for enhanced photocatalytic performance. CrystEngComm, 2021, 23, 7270-7277.	2.6	5
38	Tailoring the d-band center by borophene subunits in chromic diboride toward the hydrogen evolution reaction. Inorganic Chemistry Frontiers, 2021, 8, 5130-5138.	6.0	5
39	Enhanced electrochemical performance of the YBa0.5Sr0.5Co1.4Cu0.6O5+δ cathode material by Sm0.2Ce0.8O1.9 incorporation for solid oxide fuel cells application. Journal of Sol-Gel Science and Technology, 2020, 96, 742-752.	2.4	3
40	Raman Scattering Methods for Monitoring the Electric Properties of the Postannealed Bulk Heterojunction. ACS Applied Energy Materials, 2021, 4, 8360-8367.	5.1	1